A TRPV2–PKA Signaling Module for Transduction of Physical Stimuli in Mast Cells

Alexander J. Stokes,[1] Lori M.N. Shimoda,[1] Murielle Koblan-Huberson,[1] Chaker N. Adra,[2] and Helen Turner[1,3]

[1]*Center for Biomedical Research at the Queen's Medical Center, Honolulu, HI 96813*
[2]*Beth Israel Deaconess Medical Center, Boston, MA 02215*
[3]*Department of Cell and Molecular Biology, University of Hawaii, Honolulu, HI 96822*

Abstract

Cutaneous mast cell responses to physical (thermal, mechanical, or osmotic) stimuli underlie the pathology of physical urticarias. In vitro experiments suggest that mast cells respond directly to these stimuli, implying that a signaling mechanism couples functional responses to physical inputs in mast cells. We asked whether transient receptor potential (vanilloid) (TRPV) cation channels were present and functionally coupled to signaling pathways in mast cells, since expression of this channel subfamily confers sensitivity to thermal, osmotic, and pressure inputs. Transcripts for a range of TRPVs were detected in mast cells, and we report the expression, surface localization, and oligomerization of TRPV2 protein subunits in these cells. We describe the functional coupling of TRPV2 protein to calcium fluxes and proinflammatory degranulation events in mast cells. In addition, we describe a novel protein kinase A (PKA)–dependent signaling module, containing PKA and a putative A kinase adapter protein, Acyl CoA binding domain protein (ACBD)3, that interacts with TRPV2 in mast cells. We propose that regulated phosphorylation by PKA may be a common pathway for TRPV modulation.

Key words: calcium channels • inflammation • physical urticaria • transient receptor potential • vanilloid receptor

Introduction

Mast cells respond to multiple stimuli, including immunological inputs, polybasic secretagogues, and physical cues (1–5). Direct responsiveness to physical (thermal, osmotic, and mechanical perturbation) stimuli has been described for mast cells in vitro and in vivo (1, 3, 6–8). Mast cell responses to these physical stimuli are causative in various urticarias that derive from inappropriate activation of cutaneous mast cells (1, 9–11). Physical urticarias (PU) involve wheal-flare reactions that follow brief exposure to applied cold, heat, pressure, or light in the UVA and short-wave visible ranges (9, 12–14). These stimuli elicit release of histamine, serotonin, and other inflammatory mediators from cutaneous mast cells, causing an inflammatory reaction that is characterized by erythema, edema, and pruritis (9, 14). PU symptoms respond to H1-type antihistamines (9, 15). PU can be sporadic or may be associated with chronic (often idiopathic) urticarial disease (16). In contrast to acute allergic inflammations, an IgE–FcεRI–mediated mechanism is not widely postulated for the PU, although this may be an important component of chronic urticarial responses (16). In the absence of a clear IgE dependence for the induction of PU, it would seem important to identify a signaling mechanism that can transduce acute physical stimuli into signals that are necessary and sufficient to induce mast cell activation.

Cation channels of the transient receptor potential (vanilloid) (TRPV) family respond to various environmental inputs across both physiological and pathophysiological ranges. Six channels have been defined on the basis of similarity to the prototypical vanilloid receptor (TRPV1, VR-1) (17–20). TRPV1 was expression cloned by virtue of its ability to confer responses to the nociomimetic lipid capsaicin upon an epithelial cell line and is activated after exposure to pathophysiological temperatures (>42°C) (18, 19). TRPV2 has a higher threshold than TRPV1 for heat activation

Address correspondence to Helen Turner, Center for Biomedical Research, 1301 Punchbowl St., University Tower 8, Honolulu, HI 96813. Phone: (808) 537-7927; Fax: (808) 537-7926; email: hturner@queens.org

Abbreviations used in this paper: ACBD, Acyl CoA binding domain protein; AKAP, A kinase adapter protein; BMMC, BM-derived mast cell; PKA, protein kinase A; PKAR, PKA regulatory; PKG, protein kinase G; PU, physical urticaria; TRPV, transient receptor potential (vanilloid); VDAC, voltage-dependent anion channel.

 J. Exp. Med. © The Rockefeller University Press • 0022-1007/2004/07/137/11 $8.00
Volume 200, Number 2, July 19, 2004 137–147
http://www.jem.org/cgi/doi/10.1084/jem.20032082

(~52°C) and has no known similar sensitizing agents (17, 21). TRPV3 responds to warm temperatures (31–35°C) and is sensitized by prior temperature elevation (17, 22–24). Responsiveness to physiological temperatures (24–33°C), hypo-osmolarity, and mechanical pressure, or shear stress, have been described for TRPV4 (17, 25–27).

The expression pattern of TRPV2, 3, and 4 apparently extends beyond sensory contexts, since TRPV2 transcripts have been noted in peripheral tissues (including components of the immune system) and TRPV3/4 conductances have been described in epithelia and keratinocytes (17). TRPV2 may be involved in initiating responses to noxious temperatures in nonsensory cell types. Alternately, distinct activation mechanisms for TRPV2 may exist in these peripheral tissue contexts. Interestingly, a signaling pathway that is initiated by IGF-1 or a neuropeptide receptor can cause activation of a murine TRPV2 homologue (28–30).

We can also postulate the existence of a sensitizing mechanism for peripheral TRPV2, where a signaling event causes a decrease in the threshold temperature of the channel, bringing it into the physiological range. Such a mechanism exists for TRPV1, which gates at near physiological temperatures after cytosolic acidification or ethanol exposure (18, 31). A PKA pathway has also been proposed to regulate sensitization of TRPV1, although the components of this signaling module are unknown (32, 33). To date, a similar signaling module has not been shown to associate with or regulate TRPV2.

TRPVs confer environmental-sensing properties upon neurons and nonsensory cell types. Via TRPVs, this sensing may be coupled to calcium signals. In the current study, we hypothesized that expression of TRPVs in mast cells could confer direct sensitivity to the types of physical stimuli that activate mast cells during PU. We find various TRPV transcripts in transformed and primary mast cells. The expression and oligomerization of TRPV2 protein was confirmed in mast cells, and our data suggest that exposure to TRPV2 threshold temperatures couples to calcium entry and specific proinflammatory events. We describe a novel regulatory signaling module for TRPV2. TRPV2 apparently participates in a signaling module that comprises PKA and an adaptor protein with A kinase adapter protein (AKAP)-like properties. A PKA regulatory (PKAR) subunit binding protein, Acyl CoA binding domain protein (ACBD)3, is suggested as this adaptor that links TRPV2 and PKA. In summary, this study identifies a novel expression context, functional linkage, and regulatory signaling module for TRPV2. We conclude that TRPVs may transduce physical stimuli in mast cells, in parallel with TRPV expression in the sensory neurons with which dermal mast cells are associated. Therefore, TRPVs are potential targets for intervention in pathologies such as PU.

Materials and Methods

Cell Culture. RBL2H3 cells and HEK293 stably transfected with pcDNA6TR (Invitrogen) were maintained in DMEM/10% fetal bovine serum/2 mM glutamine in humidified 5% CO_2 at 37°C. For production of TRexHEK293 cells with inducible expression of TRPV2, parental cells were electroporated with the rat TRPV2 cDNA in pcDNA4TO. Clonal cell lines were selected by limiting dilution in 400 μg/ml zeocin (Invitrogen). TRPV2 expression was induced using 1 μg/ml tetracycline for 16 h at 37°C.

Antibodies and Reagents. Rat TRPV2 cDNA was a gift from Dr. David Julius (University of California, San Francisco, San Francisco, CA). Rabbit polyclonal anti-TRPV2 was from Calbiochem. Goat polyclonal anti-PKAR subunit was from Chemicon. Rabbit polyclonal anti-ACBD3 (34) was a gift from Dr. V. Papadopoulos (Georgetown University, Washington DC). Anti–phospho PKA substrate motif antibody was from Cell Signaling Technology. Anti-FLAG was from Sigma-Aldrich. HRP-conjugated secondary antibodies were from Amersham Biosciences. Hoechst and Alexa fluorophore–conjugated IgGs were from Molecular Probes. Lipidated, cell permeant, HT31 peptide (35) was from Promega.

RT-PCR and Electrophoresis. RT-PCR on RBL2H3 poly A^+ mRNA was performed using the following primers: (5′-3′, forward/back): TRPV1, cggctttttgggaagggtg/tgtctctgggtctttgaactcgc; TRPV2, gaacctcaacttcataaagagacctcc/ccttggtagaactcatcggtgc; TRPV3, tcaggatgatgtgacagagaccc/cagcgaaggcaagcagaatc; TRPV4, tggacggactgctctcctacttg/tcatccttgggctggaagaac; TRPV5, ccatcctccagcaaaaactactacag/gaaacgcattaggtctccaaaaatc; and TRPV6, cctttgctgcctgtgtgggtag/ttggtggtaacaataagttccagtagag.

Northern Blots. Multiple tissue and immune system Northern blots were purchased from CLONTECH Laboratories, Inc. and probed according to the manufacturer's instructions. Multiple cell line Northern blots were produced using 1 μg/lane poly A^+ mRNA. The TRPV2 cDNA probe comprised a 353-bp HincII-NotI fragment.

Immunoprecipitation and Western Blot. Cells were pelleted (2000 *g*, 2 min) and washed once in ice cold PBS. Approximately 10^7 cells were lysed (in ice for 30 min) in 350 μl of lysis buffer (50 mM Hepes, pH 7.4, 75 mM NaCl, 20 mM NaF, 10 mM iodoacetamide, 0.5% [wt/vol] Triton X-100, 1 mM PMSF, 500 μg/ml aprotinin, 1.0 mg/ml leupeptin, and 2.0 mg/ml chymostatin). Lysates were clarified (10,000 *g*, 5 min). For preparation of total protein, lysates were acetone precipitated. For immunoprecipitation, supernatants were tumbled (at 4°C for 2 h) with the indicated antibody, covalently coupled (dimethylpimelidate/ethanolamine) to protein G–Sepharose.

Samples were boiled in Laemmli buffer, resolved by SDS-PAGE, and electrotransferred to PVDF. Membranes were blocked using 5% nonfat milk or BSA (1 h at RT). Primary antibodies were incubated with membrane for 16 h at 4°C. Developing antibodies were diluted to 0.1 μg/ml and incubated with membranes for 45 min. For cell surface biotinylation, intact cells were incubated (30 min at RT) with 1 mg/ml sulfo-NHS-biotin (Pierce Chemical Co.) in PBS, pH 8.0. Cells were washed four times in PBS/25 mM NH_4Cl and then lysed/immunoprecipitated as above in the presence of 25 mM NH_4Cl.

Blue-Native Electrophoresis. Blue-Native (BN)–PAGE was adapted from Schagger and Von Jagow (36) and Schamel et al. (37). Gradient gels (6–20%) were electrophoresed in BN sample buffer (5% [wt/vol] Coomassie-G250, 100 mM Bis-Tris, pH 7.0, 500 mM 6-aminocaproic acid). Anode buffer was 50 mM Bis-Tris, pH 7.0. Cathode buffer was 50 mM tricine/15 mM Bis-Tris, pH 7.0. For the first 90 min of resolving time (100 V/1 h then 600 V/16 h), Coomassie-G250 was included in the cathode buffer at 0.02% (wt/vol). Gels were electrotransferred and Western blotted.

Immunofluorescence. Cells were fixed and permeabilized on glass coverslips (4% paraformaldehyde followed by 0.4% Triton

X-100 for 20 min at RT). After blocking (0.7% fish skin gelatin), coverslips were sequentially incubated with primary and secondary antibodies and the indicated stains. Imaging was performed with an Olympus IX70 fluorescence inverted microscope with quadruple dichroic filter block and excitation filter set 88000 (Chroma) connected to an F-view monochrome CCD camera.

Phosphorylation Assays. For metabolic labeling with $^{32}P_i$, RBL2H3 were incubated for 3 h in phosphate-free DMEM before addition of 250 μCi/ml ^{32}P orthophosphate for 4 h. Cells were harvested and then lysed as described in the Immunoprecipitation and Western Blot section. Immunoprecipitation and SDS-PAGE were performed as described in the Immunoprecipitation and Western Blot section, and the resulting gel was autoradiographed. For in vitro phosphorylation assays, dried immunocomplexes were resuspended in a buffer containing 50 mM Tris, pH 7.4, 1 mM EDTA, 12 mM $MgCl_2$, and 250 μM ATP. Additional components were added as indicated, (10 mM cAMP, 10 mM cGMP, 5 μCi $^{32}P\gamma ATP$, 1 U/μl PKA or protein kinase G [PKG] [Promega]). Reactions were incubated at 30°C for 30 min, stopped by addition of reducing sample buffer, and then resolved by SDS-PAGE.

Fura-2 Calcium Assay. RBL2H3 were loaded with 4 μM Fura-2 a.m. (Molecular Probes) in Ringer buffer with 1 mM $CaCl_2$, ~330 mOsm, for 45 min at 37°C. After washing, bulk assay of calcium flux was performed as described (38). As a positive control, cells were stimulated with thapsigargin (1 μM) or ionomycin (500 nM) in the absence and presence of external calcium (not depicted).

Serotonin Release Assay. Adherent RBL2H3 (2×10^4 cells/cm^2) were incubated with 1 μCi/ml ^3H hydroxytryptamine (New England Nuclear) for 16 h at 37°C. Monolayers were then washed once in Tyrode's buffer at 37°C, and cells were incubated with the indicated stimuli or vehicle in 250 μl/cm^2 Tyrodes buffer for 45 min at 37°C. Reactions were stopped by quenching in ice cold PBS and counted in liquid scintillation cocktail.

Results

TRPV Expression in Mast Cells. Mast cells mount intense responses to environmental cues, including thermal, osmotic, and mechanical inputs (1, 3, 11). The correlation between these stimuli and the known activation mechanisms for TRPV channels is striking (17). We hypothesized that TRPVs may mediate calcium entry into mast cells in response to certain classes of physical stimulation. We analyzed TRPV mRNA representation in the model mast cell line RBL2H3. RT-PCR reactions were performed using primer pairs designed to selectively amplify each TRPV, and TRPM7, which is an abundant conductance in RBL2H3 (39). Fig. 1 A shows that transcripts for TRPV1, 2, 4, 6, and TRPM7 may be detected in RBL2H3 cells by RT-PCR. The identity of the PCR products was confirmed by excision, purification, and sequencing.

TRPV2 transcripts are present in various tissues and the rodent mast cell lines P815 and RBL2H3 (Fig. 1 B). Using quantitative PCR, we assessed that murine BM-derived mast cells (BMMCs) and RBL2H3 contained TRPV2 transcripts at a resting level of ~10-12 pg per ng poly A^+ mRNA ($n = 3$). TRPV2 transcripts could also be detected in primary human cord blood–derived mast cells and human basophils (unpublished data). TRPV2 transcript levels in cord blood–derived mast cells are comparable with that found in primary human neutrophils, a previously defined context for TRPV2 (40).

TRPV2 Is Present in Mast Cells as a Cell Surface Oligomer with Tetrameric Stoichiometry. We sought to confirm that TRPV2 protein is present and that TRPV2 exists in mast cells as a functional, cell surface, channel oligomer. Fig. 2 A shows that anti-TRPV2 recognizes a ~90-kD protein doublet in lysates that were isolated from primary murine

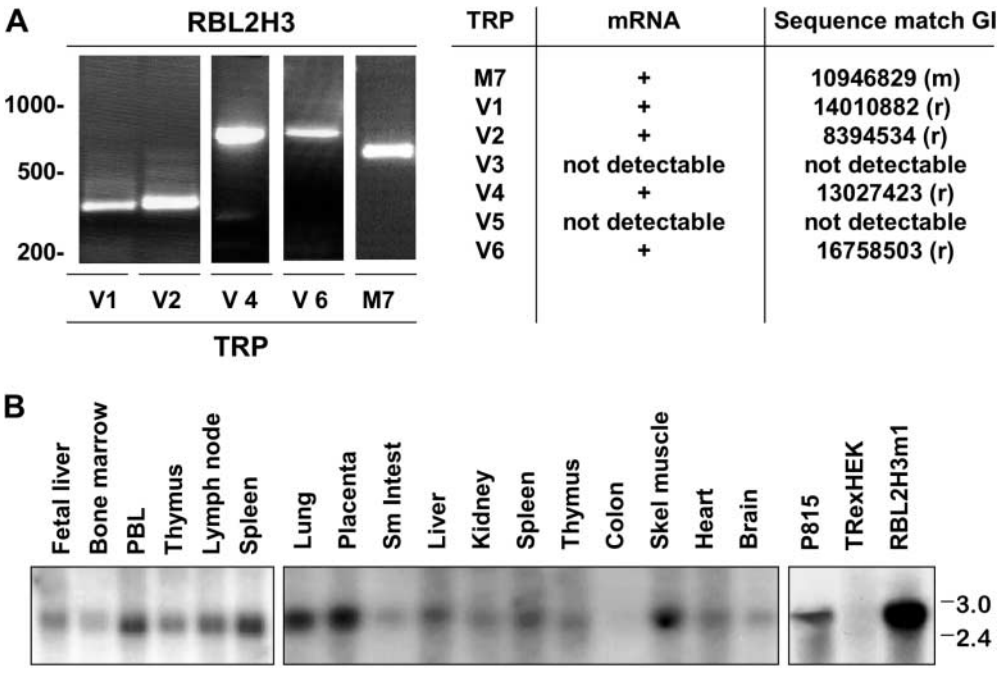

Figure 1. (A) RT-PCR analysis of TRPV expression in RBL2H3. Poly A^+ mRNA was prepared from RBL2H3 mast cells. RT-PCR using specific primers for TRPM7 and TRPV1-6. RT-PCR was performed as described in Materials and Methods. After agarose gel electrophoresis (left), specific products were excised from the gel and sequenced. BLAST analysis of sequence files was used to confirm the specificity of the PCR product (right). Results are representative of two separate primers pairs per transcript. (B) Northern blot analysis of TRPV2 expression. Multiple tissue Northern blots (left and middle; CLONTECH Laboratories, Inc.) were probed with a ^{32}P-labeled cDNA fragment corresponding to a 353-bp fragment (HincII–NotI) derived from rat TRPV2. Strong hybridization of a single band of ~2.8 kb was visible after 16-h exposure to storage phosphor screens.

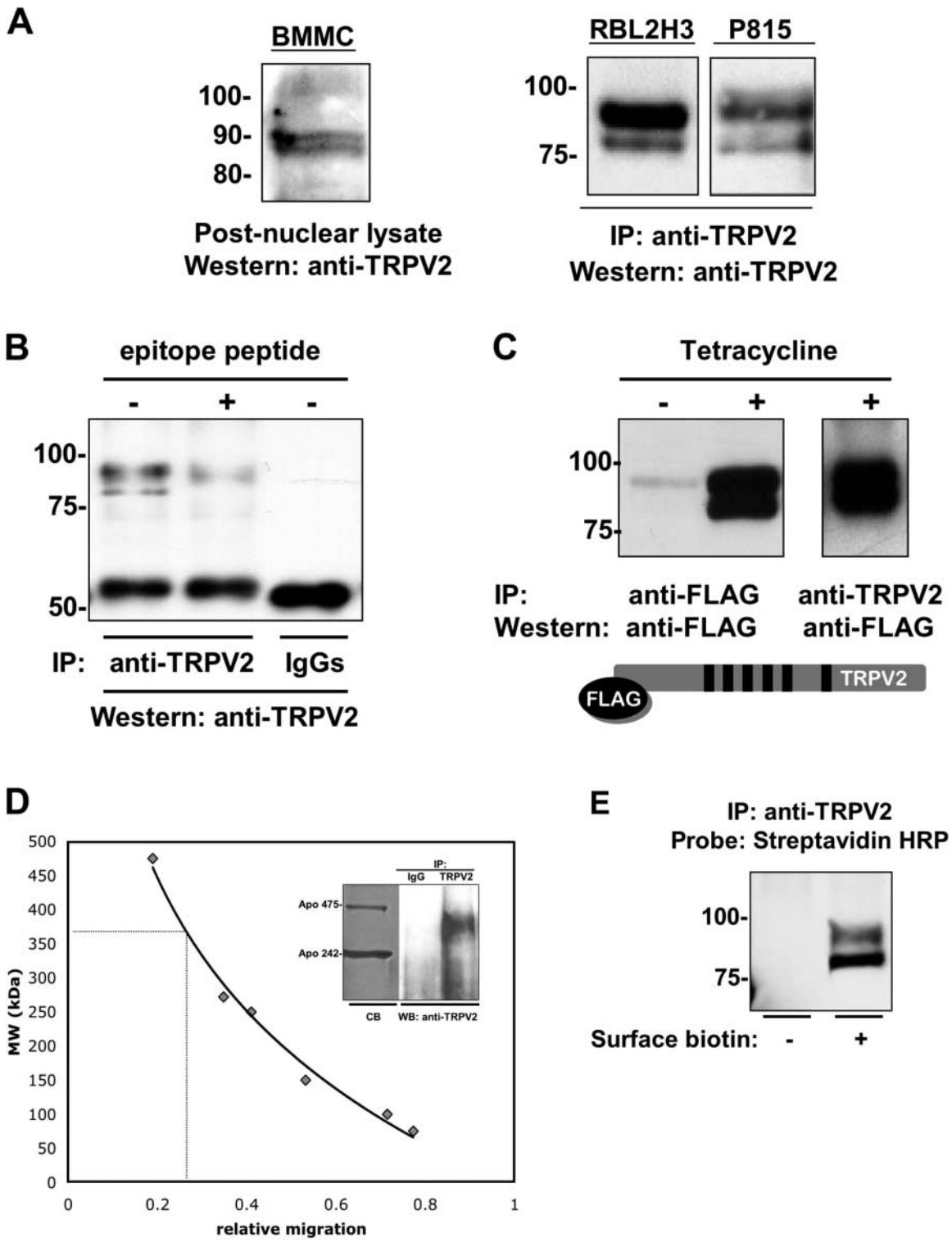

Figure 2. (A) Presence of TRPV2 protein in transformed and primary mast cells. Triton X-100 lysates were prepared from 5×10^6 murine BMMC (left) or 2×10^7 RBL2H3 or P815 cells (right). Total protein (BMMC) or anti-TRPV2 immunoprecipitates (RBL2H3, P815) were prepared as described in Materials and Methods. Proteins were resolved by 10% SDS-PAGE. TRPV2 content of the immunocomplexes was visualized via an anti-TRPV2 Western blot. (B) Incubation with TRPV2 epitope peptide diminishes the presence of the 90-kD putative TRPV2 doublet in anti-TRPV2 immunocomplexes. Triton X-100 lysates were prepared from 2×10^7 RBL2H3. Lysates were immunoprecipitated with 10 μg anti-TRPV2 or with rabbit IgGs in the absence or presence of 10 μg/ml anti-TRPV2 epitope peptide (KMSASEEDHLPLQVLQSP). Band at 55 kD corresponds to antibody heavy chain. (C) Anti-TRPV2 and anti-FLAG antibodies reciprocally immunoprecipitate FLAG-TRPV2. TRexTRPV2 cells, with FLAG-TRPV2 expression under the control of a tetracycline-sensitive transcriptional repressor, were constructed as described in Materials and Methods. TRexTRPV2 were exposed to vehicle or 1 μg/ml tetracycline for 16 h at 37°C to induce expression of FLAG-TRPV2. Triton X-100 lysates from 10^7 TRexTRPV2 cells

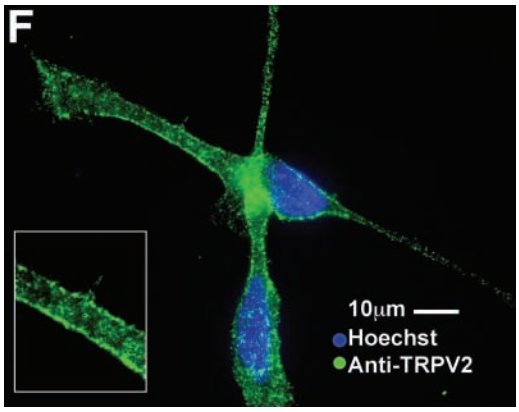

Figure 2 (continued)

were immunoprecipitated with 2 μg anti-FLAG or 10 μg anti-TRPV2. Immunocomplexes were resolved by 10% SDS-PAGE and electrotransferred. FLAG-TRPV2 was visualized by Western blotting in 0.6 μg/ml anti-FLAG antibody. (D) Native TRPV2 complexes are apparent tetramers in RBL2H3 cells. Anti-TRPV2 immunocomplexes were purified from 10^8 RBL2H3 and resolved by 6–20% gradient Blue-native electrophoresis. TRPV2 complexes were visualized by anti-TRPV2 Western blot (inset). Size determination was made relative to a Coomassie-stained gel fragment containing Apoferritin monomer (242 kD) and dimer (475 kD). Relative migration graph was plotted using R*f* values for apoferritin and recombinant protein standards (250–50-kD range). (E) TRPV2 may be surface biotinylated in RBL2H3. Intact RBL2H3 (5×10^7 cells) were surface biotinylated as described in Materials and Methods. Biotinylation reactions were quenched with 25 mM NH_4Cl. Lysates were immunoprecipitated with 10 μg anti-TRPV2, and immunocomplexes were resolved by 10% SDS-PAGE. After electrotransfer, biotinylated proteins were visualized using Streptavidin-HRP conjugate and ECL. (F) Subcellular localization of anti-TRPV2 immunofluorescence in RBL2H3. Anti-TRPV2 immunofluorescence in resting RBL2H3 was evaluated as described in Materials and Methods. Efficacy of the anti-TRPV2 in this application was verified by dual staining of TRExTRPV2 cells with anti-FLAG and anti-TRPV2 (not depicted). Anti-TRPV2 was used at 0.1 μg/ml and visualized using an Alexa-488–conjugated anti–mouse secondary antibody. Nuclei were counter stained with Hoechst 33342 (1 μg/ml). Main panel and inset show apparent plasma membrane localization of anti-TRPV2 immunoreactivity in a resting RBL2H3 cell.

BMMCs. Moreover, a similar protein doublet may be immunoprecipitated from RBL2H3 and P815 mast cells using this anti-TRPV2. Migration analysis (not depicted) suggests that these two protein species have molecular weights of 94 and 87 kD. The presence of two mobility forms of TRPV2 may indicate differential posttranslational modification, including glycosylation or phosphorylation (see Fig. 4). Specificity of the anti-TRPV2 is evidenced by the two experiments shown in Fig. 2, B and C. Fig. 2 B demonstrates that preincubation with the antigenic peptide ablates immunoprecipitation of the TRPV2 doublet. Fig. 2 C shows that the anti-TRPV2 immunoprecipitates a protein doublet from a TRexHEK cell line that expresses a FLAG epitope-tagged version of TRPV2, under the control of a tetracycline-sensitive transcriptional repressor. The same doublet may be precipitated via either the NH_2-terminal FLAG tag or the COOH-terminal anti-TRPV2 epitope.

TRP channels form functional tetramers in the plasma membrane (41). Since we are describing a novel expression context for TRPV2, we asked if the channel forms oligomers in mast cells and we assessed the subcellular localization of TRPV2. We, and others, have noted apparently detergent-resistant complexes of TRP channels, including TRPV2, even under SDS-PAGE conditions (42). It is unclear if these complexes represent physiological oligomers, and they cannot be sized accurately by conventional SDS-PAGE. Therefore, we employed a blue-native electrophoresis system to analyze the oligomerization of TRPV2. Blue-native electrophoresis uses aminocaproic acid and Coomassie dye to solubilize and charge-shift large membrane protein complexes, respectively (36, 37). Native TRPV2 complexes purified from RBL2H3 (Fig. 2 D) migrate in this system at a molecular weight (375 kD) that is consistent with the tetrameric stoichiometry that has been demonstrated for TRPVs 1, 5, and 6 (42–44). Similar oligomers are present in the TRexTRPV2 cells, although an abundant monomeric population also appears as a presumable result of overexpression (unpublished data).

We were able to surface biotinylate TRPV2 in a resting population of RBL2H3 (Fig. 2 E). To assess the proportion of RBL2H3 that this surface labeling represented, we performed fluorescence immunocytochemistry. Anti-TRPV2 immunoreactivity is present at the cell periphery in a subpopulation (10–20%) of resting RBL2H3 (Fig. 2 F). Together, these data suggest that TRPV2 protein is expressed in transformed and primary mast cells. Moreover, the configuration and localization of mast cell TRPV2 are consistent with our expectations for a functional channel.

Functionally Coupled Responses to Noxious Temperatures in Mast Cells. TRPV2 activates at 50°C, a temperature that elicits heat urticaria when used as a diagnostic challenge, in both endogenous (e.g., mammalian neurons) and overexpression systems (HEK cells or *Xenopus* oocytes). Prior to the cloning of TRPV2, heat-induced currents had been described in sensory neurons, and careful analysis of membrane integrity in these studies revealed that certain irreversible membrane events occur only when temperatures of >59–60°C are attained (45). We assessed cell viability and proliferative capability of RBL2H3 and HEK 293 after both ramped and transient temperature elevation protocols. When peak temperatures were <57–58°C, we did not observe detrimental acute effects on membrane integrity (assayed via Trypan blue exclusion) or proliferative ability of the cells (unpublished data).

We asked if transient elevation to the TRPV2 threshold temperature caused secretion of proinflammatory mediators from RBL2H3 mast cells. Fig. 3 A shows that ligation of the FcεRI at 37°C induces serotonin release in RBL2H3 and that this release depends on the presence of external calcium during the stimulation period. Similarly, transient elevation to a peak temperature of 51°C but not 45°C evokes serotonin release that is also dependent on the presence of extracellular calcium. Secretory responses evoked by immunoreceptor stimulation and heat transients are both sensitive to the inhibitor ruthenium red, which has been shown to block TRPV channels, including TRPV2 (Fig. 3 B; references 21, 46). These data imply that brief elevation to the TRPV2

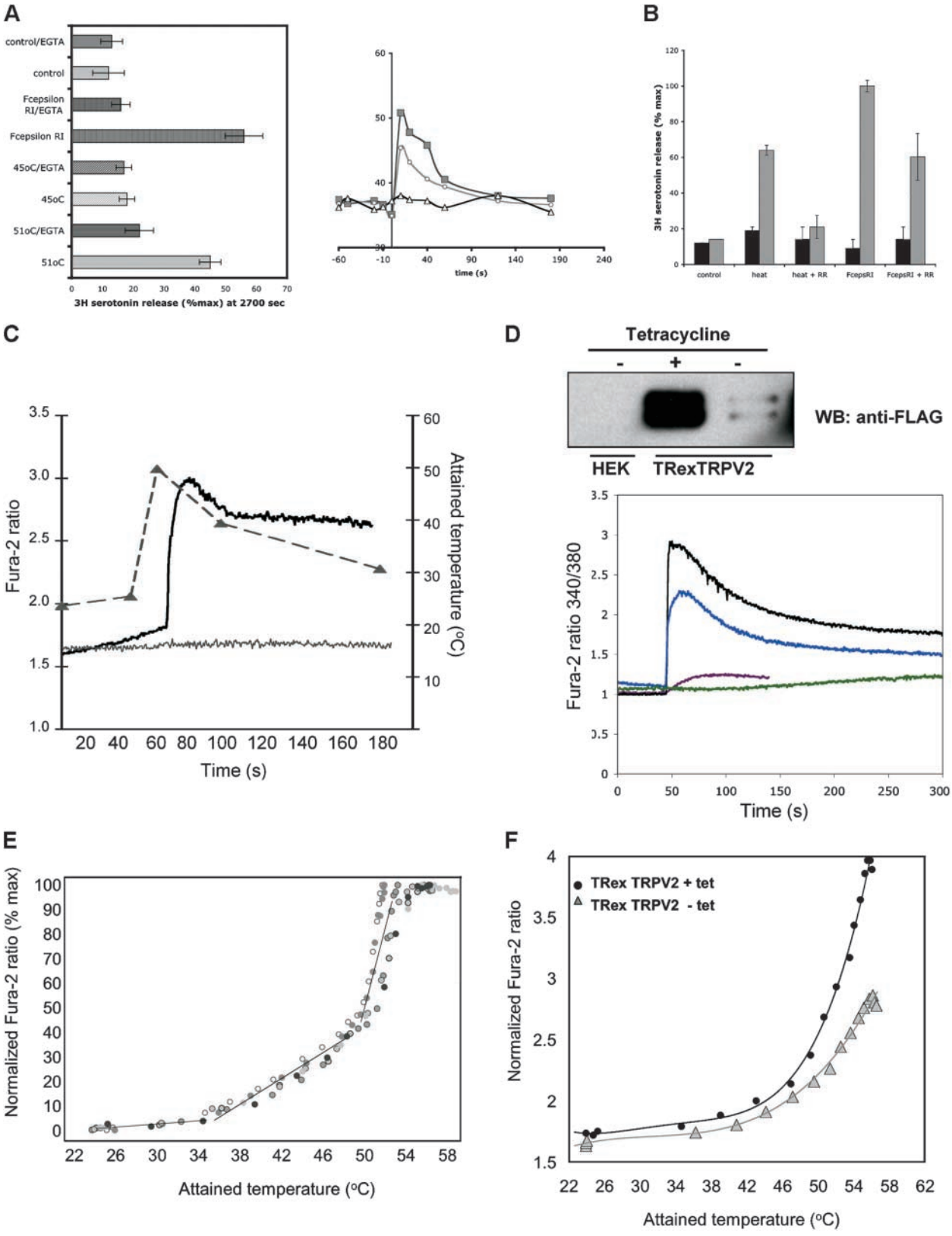

Figure 3. (A) Extracellular calcium-dependent degranulation of mast cells after temperature elevation or antigen stimulation. RBL2H3 were cultured for 24 h in ^{3}H-serotonin. For subsequent FcεRI stimulations, RBL2H3 were primed with 1 μg/ml IgE anti-DNP for 16 h. Stimulations were performed in Tyrode's buffer (1 mM $CaCl_2$) in the presence or absence of EGTA, as indicated, at 37°C. FcεRI was cross-linked using 100 ng/ml DNP-BSA. Temperature elevations were achieved via application of heated isotonic buffer, and the monitored temperature profiles are shown in the right panel. Serotonin release was assayed 45 min after stimulation and expressed as a percentage of the maximal signal obtained when RBL2H3 were exposed to a 100 nM

threshold temperature initiates a calcium influx pathway that couples to the degranulation mechanism in mast cells.

Transient temperature elevation causes significant calcium mobilization in RBL2H3. In Fig. 3 C, the temperature profile and Fura-2 signal were monitored simultaneously in RBL2H3 after application of a heated isotonic buffer. Rapid temperature elevation resulted in a marked increase in intracellular calcium levels, which declined rapidly on cooling (Fig. 3 C). Similar calcium responses were observed in TRexTRPV2 cells. Responsiveness to TRPV2 threshold temperatures was conferred upon wild-type HEK cells by TRPV2 transfection, and the magnitude of the heat-evoked calcium signal correlated positively with the degree of TRPV2 protein expression (Fig. 3 D). We also noted a variable degree of sensitivity of these calcium responses to Ruthenium red and $LaCl_3$ (unpublished data).

We applied ramped temperature increases to RBL2H3 and simultaneously monitored the attained temperature and Fura-2 fluorescence. Fig. 3 E shows the Fura-2 profile of multiple individual temperature ramps ($n = 8$) normalized to the attained temperature. At temperatures between 24 and 33°C, no significant increase in Fura-2 fluorescence is observed. Through the 34–49°C range, the Fura-2 signal increases at a mean rate of 0.09 intensity unit $°C^{-1}$ (± 0.013 U $°C^{-1}$, $n = 8$). In the 49–54°C range, Fura-2 signal increases at a mean rate of 0.32 intensity unit/°C (± 0.09 U $°C^{-1}$, $n = 8$). Thus the rate of calcium increase in these cells increases significantly ($P < 0.0001$) at two discrete points in the temperature ramp. The temperature/Fura-2 signal relationship in these cells is therefore consistent with the sequential opening of multiple channel species that have distinct threshold temperatures. We asked if such temperature/Fura-2 signal relationships could detect enhanced expression of a single channel species. We performed ramped temperature increases in TRexTRPV2 cells (Fig. 3 F). In cells with minimal TRPV2 expression, the Fura-2 signal increases at a rate of 0.0004, 0.004, and 0.007 $U°C^{-1}$ between the temperatures of 22–38°C, 34–48°C, and 48–56°C, respectively. In cells with marked overexpression of TRPV2, the latter rate increases to 0.019 $U°C^{-1}$.

TRPV2 Is a Substrate for PKA-mediated Phosphorylation. We reasoned that analysis of the protein–protein interactions made by TRPV2 might give us insight into potential regulatory mechanisms that would be applicable to both mast cell and central nervous system expression contexts for TRPV2. PKA directly phosphorylates TRPV1 and the heat-sensitive potassium channel TREK (32, 33, 47), and in both cases, this phosphorylation modulates the electrophysiological properties of the channel. We asked if TRPV2 was also a substrate for regulatory phosphorylation via PKA in mast cells. We first established that PKA but not PKG could mediate the in vitro phosphorylation of TRPV2 (Fig. 4 A).

In vitro phosphorylation assays show that a particular kinase is capable of phosphorylating a substrate such as TRPV2, but they do not show that this is a physiological event. We asked if endogenous TRPV2 is a phosphoacceptor. Fig. 4 B shows that the TRPV2 protein that was immunoprecipitated from $^{32}P_i$-labeled cells shows phosphate incorporation. In addition, Western blot analysis suggested that TRPV2 from RBL2H3 cells is recognized by antibodies raised against phospho-threonine (unpublished data) and by an antibody raised against a phosphorylated PKA substrate motif consensus peptide (Fig. 4 C). Recognition of TRPV2 by this antibody increases when the cell population is exposed to forskolin. Together, these data suggest that TRPV2 is indeed a PKA substrate and that PKA phos-

PMA, 500 ng/ml ionomycin ($n = 3$). (B) Ruthenium red blocks degranulation of mast cells after temperature elevation or antigen stimulation. Serotonin release assay was performed as described in Materials and Methods with the addition of 250 nM ruthenium red 5 min before stimulation in the indicated samples. The maximum attained temperature in this experiment was 52.4°C, and temperature returned to 37°C within 200 s. Black and gray bars show ^{3}H-serotonin levels in extracellular buffer at 30 and 2,700 s after addition of stimuli, respectively. (C) Transient elevation to the TRPV2 threshold temperature causes calcium mobilization in RBL2H3. RBL2H3 were resuspended in Ringer buffer (containing 1 mM $CaCl_2$) at a concentration of 5×10^6 cells/ml and loaded with 4 μM Fura-2 a.m. for 30 min at 37°C. Cells were equilibrated in a 25°C cuvette for the first 40 s recording time. (Heavy trace) Heated isotonic buffer was applied at 40 s, and the resulting temperature profile is shown in the overlaid broken line. Temperature peaked at 50.1°C and declined to 27°C during the recording period. (Light trace) Isotonic Ringer buffer (24°C) was added to the cuvette at 40 s and the Fura-2 signal was recorded over time. (D) Transient elevation to the TRPV2 threshold temperature causes calcium mobilization in TRExTRPV2 cells. TRExTRPV2 cells were incubated in the absence or presence of 1 μg/ml tetracycline for 16 h at 37°C. (Left) Relative expression levels of FLAG-TRPV2 in uninduced and induced TRExTRPV2 cells. Anti-FLAG immunoprecipitates were harvested from the indicated cells (parental HEK and TRexTRPV2 transfectants) and resolved by 10% SDS-PAGE. Levels of FLAG-TRPV2 were visualized by anti-FLAG Western blot. (Right) Calcium mobilization after temperature elevation in TRExTRPV2 and HEK cells. Cells were resuspended in Ringer buffer (containing 1 mM $CaCl_2$) at a concentration of 5×10^6 cells/ml and loaded with 4 μM Fura-2 a.m. for 30 min at 37°C. Cells were equilibrated in a 25°C cuvette for the first 40 s recording time. (Black trace) TRExTRPV2 cells after tetracycline induction. Heated isotonic buffer was applied at 40 s. Maximum attained temperature was 52.8°C. (Blue trace) TRExTRPV2 cells without tetracycline induction. Heated isotonic buffer was applied at 40 s. Maximum attained temperature was 54.9°C. (Purple trace) Wild-type HEK cells. Heated isotonic buffer was applied at 40 s. Maximum attained temperature was 53.9°C. (Green trace) TRExTRPV2 cells after tetracycline induction. Isotonic Ringer buffer (24°C) was added to the cuvette at 40 s, and the Fura-2 signal was recorded over time. (E) Relationship between Fura-2 signal intensity and attained temperature in RBL2H3. RBL2H3 were resuspended in Ringer buffer (containing 1 mM $CaCl_2$) at a concentration of 5×10^6 cells/ml and loaded with 4 μM Fura-2 a.m. for 30 min at 37°C. The Fura-2 signal and attained temperature were monitored simultaneously during heat ramps (mean rate of heating, $0.4°Cs^{-1}$). The seven individual traces presented here have been normalized to the time course. Shaded area highlights three distinct phases of calcium mobilization that occur consistently throughout distinct experiments. The following mean (±SD) rates of increase in Fura-2 signal were calculated for seven datasets: 24–33°C, no significant increase in Fura-2 fluorescence is observed; 34–49°C, 0.09 intensity unit $°Cs^{-1}$ (± 0.013 U $°Cs^{-1}$, $n = 8$). In the 49–54°C range, Fura-2 signal increases at a mean rate of 0.32 intensity unit/°C (± 0.09 U $°Cs^{-1}$, $n = 8$). (F) Relationship between Fura-2 signal intensity and attained temperature in TRExTRPV2 cells. TRExTRPV2 cells were incubated in the absence or presence of 1 μg/ml tetracycline for 16 h at 37°C (see panel D for expression data). Cells were resuspended in Ringer buffer (containing 1 mM $CaCl_2$) at a concentration of 5×10^6 cells/ml and loaded with 4 μM Fura-2 a.m. for 30 min at 37°C. The Fura-2 signal and attained temperature were monitored simultaneously during heat ramps (mean rate of heating $0.31°Cs^{-1}$ + tet, $0.41°Cs^{-1}$ − tet).

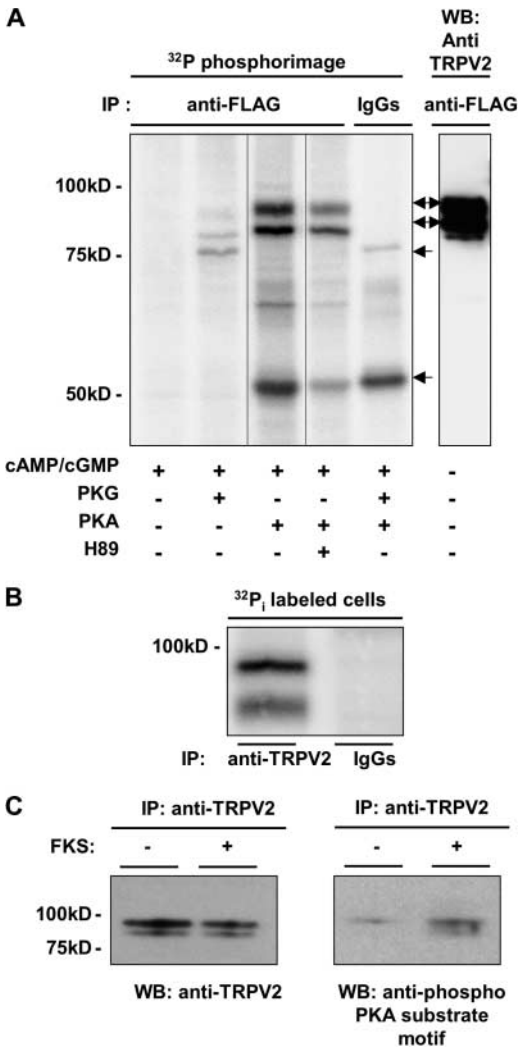

Figure 4. (A) TRPV2 is a substrate for in vitro phosphorylation by the cAMP-dependent kinase (PKA). TRexTRPV2 cells were treated with 1 μg/ml tetracycline for 16 h. Lysates were immunoprecipitated with 2 μg anti-FLAG or IgGs. Immunocomplexes were resuspended in a kinase assay buffer with 10 μM cAMP/cGMP, 1 U/μl PKA or PKG, 10 μM H89, as indicated, and 5 μCi ^{32}P-γATP. Immunocomplexes were resolved by 10% SDS-PAGE and transferred to PVDF. A duplicate gel was produced for anti-FLAG Western analysis (right). Phosphate incorporation into the 90-kD protein doublet corresponding to TRPV2 (double arrows) was evaluated by exposure to storage phosphor screens for 4.5 h. Bottom arrow marks position of autophosphorylated PKA catalytic subunit, whereas autophosphorylated protein kinase G is apparent at 78 kD ($n = 3$). All lanes in the left panel are derived from the same gel and are at same contrast. Order of lanes was altered digitally. (B) TRPV2 is a phosphoacceptor. RBL2H3 were metabolically labeled with ^{32}P-orthophosphate as described in Materials and Methods. Triton X-100 lysates were prepared from 4×10^7 cells and immunoprecipitated with 10 μg anti-TRPV2. Immunocomplexes were resolved by 7.5% SDS-PAGE and transferred to PVDF. The ^{32}P content of anti-TRPV2 immunocomplexes was assessed by exposure of the membrane to a storage phosphor screen for 24 h ($n = 2$). (C) TRPV2 recognition by a phospho-PKA substrate motif antibody increases after forskolin treatment. RBL2H3 were treated with vehicle or 25 μM forskolin for the 10 min at 37°C. Triton X-100 lysates were prepared from 4×10^7 cells and immunoprecipitated with 20 μg anti-TRPV2. After 10% SDS-PAGE and electrotransfer, duplicate Western blots were probed with either anti-TRPV2 (left) or an antibody raised against a phosphorylated consensus PKA substrate motif (right).

phorylation of TRPV2 occurs in resting cells but may be enhanced by cAMP mobilization.

TRPV2 Associates Directly with PKARII in Mast Cells Via an AKAP. The PKA-mediated phosphorylation of TRPV2 suggests that the channel is part of a signaling complex that contains PKA. We detected a protein species in anti-TRPV2 immunocomplexes that is immunoreactive with antibodies raised against the PKARII PKAR subunit (Fig. 5 A).

PKA enzymes rarely associate directly with their substrate. Specific AKAPs are used to target PKA to a particular substrate (33, 48). A PKA–AKAP signaling module has been proposed to interact with TRPV1, but the identity of any TRP-associated AKAP remains unknown (33). We asked if an AKAP species was likely to mediate the interaction between PKA and TRPV2. We used a cell-permeant form of the HT31 peptide (35), which is predicted to block the interaction between AKAPs and PKAR. HT31 exploits the fact that a conserved secondary structural motif, an amphipathic α-helical region, is the contact area between the known AKAPs and PKAR subunits. Fig. 5 A shows that HT31 blocks association between TRPV2 and PKARII, implying that a specific AKAP bridges TRPV2 and PKA.

The PKA-binding Protein ACBD3 May Mediate the TRPV2–PKA Interaction. The ACBD3 protein (formerly PAP7) binds PKARIα and apparently recruits PKA to the peripheral benzodiazepine receptor (34, 49). Our yeast two-hybrid data (unpublished data) suggested that ACBD3 may bind to the NH_2 terminus of TRPVs, and we proposed that ACBD3 might link TRPV2 and the PKAR subunit. Northern (not depicted) and Western analysis suggests that ACBD3 is widely expressed and is an abundant protein in the mast cell lines tested here (Fig. 5 B). Fig. 5 C shows that anti-TRPV2 immunocomplexes from RBL2H3 contain ACBD3. This interaction is unaffected by the HT31 peptide. Fig. 5 D shows that the presence of ACBD3 in anti-TRPV2 immunoprecipitates is due to the primary immunoprecipitation of TRPV2.

We asked if ACBD3 indeed interacted with the PKAR subunit in RBL2H3. RBL2H3 express both PKARI and PKARII (not depicted). Fig. 5 E shows that anti-PKARIIα immunoprecipitates purified from RBL2H3 contain ACBD3. The presence of ACBD3 in PKARIIα immunocomplexes is reduced in cells pretreated with a membrane-permeant form of the HT31 peptide, indicating an AKAP-like interaction. We were not able to capture ACBD3 or PKARI immunocomplexes from RBL2H3 with the available antibodies, and therefore we cannot assess whether ACBD3 associates with PKARIα.

Discussion

This work describes a novel expression context and regulatory signaling module for TRPV2. The initial description of TRPV2 (17, 21) suggested a wide distribution of its transcripts, for example, in leukocytes an observation that seems inconsistent with a narrow definition of its function

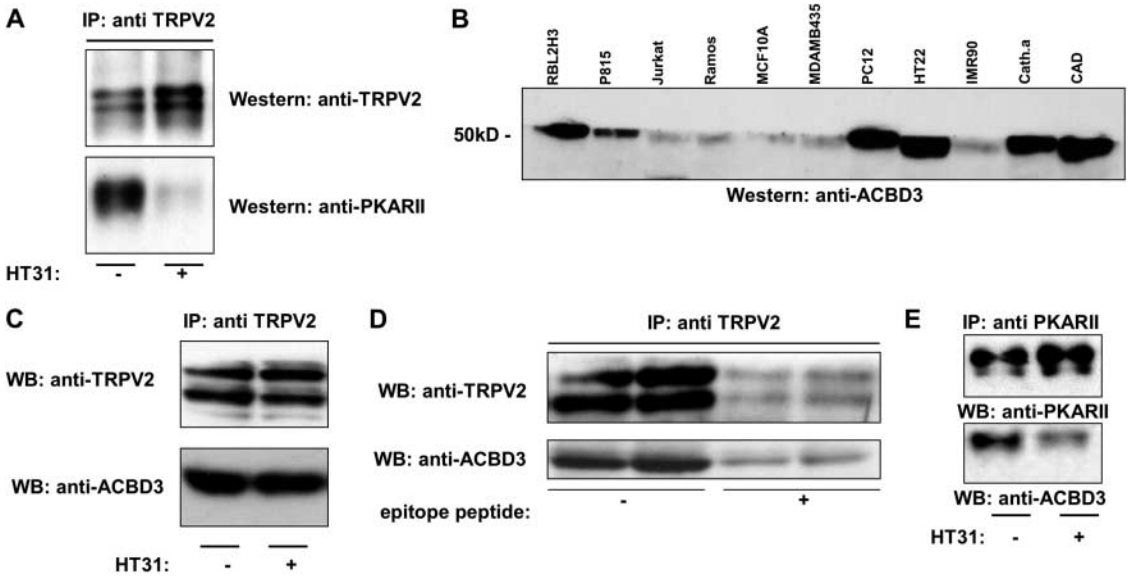

Figure 5. (A) TRPV2 associates with the PKAR subunit via an AKAP. Triton X-100 lysates were prepared from 5×10^7 RBL2H3. Lysates were immunoprecipitated with 10 μg anti-TRPV2 in the absence or presence of 50 μM HT31 peptide. Immunocomplexes were resolved by 10% SDS-PAGE and transferred to PVDF. The membrane was sequentially probed with either anti-TRPV2 or the goat polyclonal anti-PKARII (1 μg/ml). (B) Western blot analysis of ACBD3 expression. Triton X-100 lysates were prepared from 5×10^6 cells from the indicated cell lines. Total protein was harvested from these samples by acetone precipitation, and protein levels were normalized using a Bradford assay. Samples were resolved by 10% SDS-PAGE and Western blotted using 2 μg/ml of the rabbit polyclonal anti-ACBD3. The cell lines tested represent the following backgrounds: P815/RBL2H3, mast; Ramos, B lymphocyte; jurkat, T lymphocyte; MCF10A/MDAMB435, epithelial fibroblast; PC12, phaeochromocytoma; HT22, neuron; IMR90, fibroblast; Cath.a/CAD, neuron. (C) Co-immunoprecipitation of TRPV2 and ACBD3. Triton X-100 lysates were prepared from 5×10^7 RBL2H3. Lysates were immunoprecipitated with 10 μg anti-TRPV2 in the absence or presence of 50 μM HT31 peptide. Immunocomplexes were resolved by 10% SDS-PAGE and transferred to PVDF. The membrane was divided and probed separately with either anti-TRPV2 or anti-ACBD3 ($n = 3$). (D) Epitope peptide competition of TRPV2–ACBD3 interaction. Triton X-100 lysates were prepared from 5×10^7 RBL2H3. Lysates were immunoprecipitated with 10 μg anti-TRPV2 in the absence or presence of 20 μg/ml TRPV2 epitope peptide. Immunocomplexes were resolved by 10% SDS-PAGE and transferred to PVDF. The membrane was divided and probed separately with either anti-TRPV2 or anti-ACBD3 ($n = 3$). (E) Co-immunoprecipitation of PKARII and ACBD3. Triton X-100 lysates were prepared from 5×10^7 RBL2H3. Lysates were immunoprecipitated with 10 μg of goat polyclonal anti-PKARII in the absence or presence of 50 μM HT31 peptide. Immunocomplexes were resolved by 7.5% SDS-PAGE and transferred to PVDF. The membrane was probed sequentially with anti-PKARII and anti-ACBD3 ($n = 3$).

as a sensor of pathologically high temperatures. Our current study supports the concept that TRPV2 protein is not restricted to the central nervous system. In mast cells, at least, there is the potential for a direct linkage between the known activation mechanism of TRPV2 and a functional outcome. We propose that TRPVs, including TRPV2, may mediate calcium entry in response to physical stimulation of mast cells and that this mechanism is a component of the signaling pathway that drives inflammatory responses to physical inputs. The concept of a direct sensor for physical stimuli in mast cells is supported by previous in vitro studies, where mast cells were exposed to physical stimuli in the absence of any local sensory neurons (1, 6–8, 11) and is suggested by the presence of TRPVs. However, it is also likely that sensory neurons, also expressing TRPVs, may contribute indirectly to the control of mast cell activation in response to physical stimuli, for example, via release of nerve growth factor, which can induce mast cell activation (56). The interplay between these mechanisms remains to be elucidated.

Mast cell TRPVs may contribute to PU where physical stimuli elicit wheal-flare reactions that are driven by cutaneous mast cells. Heat urticaria is evoked diagnostically by brief exposure of skin to temperatures of 45–55°C, a stimulus that would be predicted to activate the TRPV1 and/or TRPV2 channels that may be present in cutaneous mast cells (50). Our data show that these stimuli can be functionally coupled to inflammatory mediator release in a model mast cell line. Future work may also reveal other functional linkages between physical stimuli, urticarial responses, and TRPVs in cutaneous mast cells. For example, dermatographism is a specific PU where mast cell–dependent wheal-flare reactions follow brief pressure to the dermis (9, 10, 14), whereas the diagnostic criterion for cold urticaria is the appearance of highly localized hives within a few minutes of cutaneous exposure to temperatures of 4–14°C. Transcripts for the pressure-activated TRPV4 and a potentially cold-gated TRP channel are present in model mast cells (unpublished data). Expression of a range of TRPV-type sensors, if they can be shown to couple to functionally significant downstream signaling pathways, may therefore confer sensitivity to a spectrum of physical stimuli. In addition to the potential for contribution to PU, it is possible that direct sensing of noxious physical stimuli by mast cells plays a role in the inflammatory responses that follow thermal wounding (3, 51).

Activating stimuli, but not necessarily activation mechanisms, have been described for TRPVs. An activation mechanism that involves direct physical sensing by the TRPV is apparently precluded by recent data showing that excised membrane patches containing TRPV4 do not retain responsiveness to activating temperatures for this channel (26). It seems likely that a second messenger-based signaling system is involved, and the diverse apparent regulation of TRPVs by lipid mediators may provide insight into this issue (17). The presence of a sensitizing mechanism could be important in understanding the role of TRPv2 in seemingly paradoxical, nonsensory expression contexts (e.g., lymphocytes). A PKA-mediated sensitization mechanism has been defined previously for TRPV1 and the heat-activated K^+ channel, TREK. Our data suggest that a PKA signaling module acts directly on TRPV2. Future work will reveal which properties of the channel are affected by PKA phosphorylation. We observe a potentiation in heat-evoked calcium responses in forskolin-treated RBL2H3, which may reflect A kinase–dependent modulation of TRPV2 channels (unpublished data). However, there may be considerable complexity in the relationship between PKA and TRPV2, since we can identify a regulated surface localization step (29, 30) in TRPV2 biosynthesis that is cAMP regulated (unpublished data). Therefore, forskolin potentiation of TRPV2 responses could be an effect of increased channel density at the cell surface.

We have identified a novel signaling protein that associates with TRPV2, the PKAR binding protein ACBD3 (49). This interaction is not exclusive, since ACBD3 has been described as an adaptor protein in the context of a mitochondrial complex that is assembled around the voltage-dependent anion channel (VDAC) (34, 49). ACBD3 interacts with VDAC via an intermediary protein, the peripheral benzodiazepine receptor (34, 49). We cannot yet state whether the TRPV2–ACBD3 interaction is direct. In both TRPV2 and VDAC contexts, however, it appears that the role of ACBD3 is to recruit PKA into the channel microenvironment. ACBD3 appears to fulfill some of the functional criteria for classification as an AKAP. However, recruitment of the PKA catalytic subunit by ACBD3 has not been demonstrated in either system. AKAPs are proposed to contain a common structural motif, an amphipathic a-helix that mediates complex formation between the AKAP and PKAR subunit. We can identify several such motifs in the ACBD3 COOH terminus using helical wheel analysis (not depicted). Future mutational analysis will determine whether ACBD3 is indeed using this helical motif to interact with PKAR. It is clear that a PKA signaling module affects the activation properties of TRPV1, apparently contributing to the desensitization process (32, 33). Together with our present data, this observation raises the question of whether an ACBD3–PKA module is common to both TRPV1 and TRPV2. To date, we have not been able to coprecipitate TRPV1 and ACBD3.

In summary, the present study suggests that TRPV cation channels, including TRPV2, may contribute to mast cell physiology and potentially to pathologies that result from inappropriate mast cell activation in response to physical stimuli. Regulation by cAMP/PKA signaling pathways may be a recurring theme among TRPV species and may affect TRPV functionality at multiple levels.

The authors thank Clay Wakano and Linden Doescher for providing excellent technical assistance and Drs. Stephen J. Galli and Sakhura Nakahara (Stanford University) and Dr. Jean-Pierre Kinet (Harvard Medical School) for sharing unpublished data. We thank the Greenwood Molecular Biology Facility of the University of Hawaii for providing DNA sequencing and quantitative PCR facilities.

The authors acknowledge the support of the Charles E. Culpeper Biomedical Pilot Initiative (grant to H. Turner).

Submitted: 3 December 2003
Accepted: 28 May 2004

References

1. Church, M.K., Y. Okayama, and S. el-Lati. 1991. Mediator secretion from human skin mast cells provoked by immunological and non-immunological stimulation. *Skin Pharmacol.* 4:15–24.
2. Galli, S.J. 2000. Mast cells and basophils. *Curr. Opin. Hematol.* 7:32–39.
3. Noli, C., and A. Miolo. 2001. The mast cell in wound healing. *Vet. Dermatol.* 12:303–313.
4. Metcalfe, D.D., D. Baram, and Y.A. Mekori. 1997. Mast cells. *Physiol. Rev.* 77:1033–1079.
5. Sharma, B.B., J.R. Apgar, and F.T. Liu. 2002. Mast cells. Receptors, secretagogues, and signaling. *Clin. Rev. Allergy Immunol.* 22:119–148.
6. Eggleston, P.A., A. Kagey-Sobotka, and L.M. Lichtenstein. 1987. A comparison of the osmotic activation of basophils and human lung mast cells. *Am. Rev. Respir. Dis.* 135:1043–1048.
7. Fredholm, B., and O. Hagermark. 1970. Studies on histamine release from skin and from peritoneal mast cells of the rat induced by heat. *Acta Derm. Venereol.* 50:273–277.
8. Silber, G., D. Proud, J. Warner, R. Naclerio, A. Kagey-Sobotka, L. Lichtenstein, and P. Eggleston. 1988. In vivo release of inflammatory mediators by hyperosmolar solutions. *Am. Rev. Respir. Dis.* 137:606–612.
9. Grabbe, J. 2001. Pathomechanisms in physical urticaria. *J. Investig. Dermatol. Symp. Proc.* 6:135–136.
10. Soter, N.A., and F. Austen. 1977. Urticaria, angioedema, and mediator release in humans in response to physical environmental stimuli. *Fed. Proc.* 36:1736–1741.
11. Soter, N.A., and S.I. Wasserman. 1980. Physical urticaria/angioedema: an experimental model of mast cell activation in humans. *J. Allergy Clin. Immunol.* 66:358–365.
12. Claudy, A. 2001. Cold urticaria. *J. Investig. Dermatol. Symp. Proc.* 6:141–142.
13. Daman, L., P. Lieberman, M. Ganier, and K. Hashimoto. 1978. Localized heat urticaria. *J. Allergy Clin. Immunol.* 61:273–278.
14. Greaves, M.W. 1991. The physical urticarias. *Clin. Exp. Allergy.* 21:284–289.
15. Merk, H.F. 2001. Standard treatment: the role of antihistamines. *J. Investig. Dermatol. Symp. Proc.* 6:153–156.
16. Greaves, M.W. 2003. Chronic idiopathic urticaria. *Curr. Opin. Allergy Clin. Immunol.* 3:363–368.
17. Benham, C.D., M.J. Gunthorpe, and J.B. Davis. 2003. TRPV channels as temperature sensors. *Cell Calcium.* 33:479–487.

18. Caterina, M.J., M.A. Schumacher, M. Tominaga, T.A. Rosen, J.D. Levine, and D. Julius. 1997. The capsaicin receptor: a heat-activated ion channel in the pain pathway. *Nature*. 389:816–824.
19. Julius, D., and A.I. Basbaum. 2001. Molecular mechanisms of nociception. *Nature*. 413:203–210.
20. Nilius, B. 2003. From TRPs to SOCs, CCEs and CRACs: consensus and contraversies. *Cell Calcium*. 33:293–298.
21. Caterina, M.J., T.A. Rosen, M. Tominaga, A.J. Brake, and D. Julius. 1999. A capsaicin-receptor homologue with a high threshold for noxious heat. *Nature*. 398:436–441.
22. Peier, A.M., A.J. Reeve, D.A. Andersson, A. Moqrich, T.J. Earley, A.C. Hergarden, G.M. Story, S. Colley, J.B. Hogenesch, P. McIntyre, et al. 2002. A heat-sensitive TRP channel expressed in keratinocytes. *Science*. 296:2046–2049.
23. Smith, G.D., M.J. Gunthorpe, R.E. Kelsell, P.D. Hayes, P. Reilly, P. Facer, J.E. Wright, J.C. Jerman, J.P. Walhin, L. Ooi, et al. 2002. TRPV3 is a temperature-sensitive vanilloid receptor-like protein. *Nature*. 418:186–190.
24. Xu, H., I.S. Ramsey, S.A. Kotecha, M.M. Moran, J.A. Chong, D. Lawson, P. Ge, J. Lilly, I. Silos-Santiago, Y. Xie, et al. 2002. TRPV3 is a calcium-permeable temperature-sensitive cation channel. *Nature*. 418:181–186.
25. Guler, A.D., H. Lee, T. Iida, I. Shimizu, M. Tominaga, and M. Caterina. 2002. Heat-evoked activation of the ion channel, TRPV4. *J. Neurosci*. 22:6408–6414.
26. Watanabe, H., J. Vriens, S.H. Suh, C.D. Benham, G. Droogmans, and B. Nilius. 2002. Heat-evoked activation of TRPV4 channels in a HEK293 cell expression system and in native mouse aorta endothelial cells. *J. Biol. Chem*. 277:47044–47051.
27. Alessandri-Haber, N., J.J. Yeh, A.E. Boyd, C.A. Parada, X. Chen, D.B. Reichling, and J.D. Levine. 2003. Hypotonicity induces TRPV4-mediated nociception in rat. *Neuron*. 39: 497–511.
28. Boels, K., G. Glassmeier, D. Herrmann, I.B. Riedel, W. Hampe, I. Kojima, J.R. Schwarz, and H.C. Schaller. 2001. The neuropeptide head activator induces activation and translocation of the growth-factor-regulated Ca(2+)-permeable channel GRC. *J. Cell Sci*. 114:3599–3606.
29. Iwata, Y., Y. Katanosaka, Y. Arai, K. Komamura, K. Miyatake, and M. Shigekawa. 2003. A novel mechanism of myocyte degeneration involving the Ca2+-permeable growth factor-regulated channel. *J. Cell Biol*. 161:957–967.
30. Kanzaki, M., Y.Q. Zhang, H. Mashima, L. Li, H. Shibata, and I. Kojima. 1999. Translocation of a calcium-permeable cation channel induced by insulin-like growth factor-I. *Nat. Cell Biol*. 1:165–170.
31. Trevisani, M., D. Smart, M.J. Gunthorpe, M. Tognetto, M. Barbieri, B. Campi, S. Amadesi, J. Gray, J.C. Jerman, S.J. Brough, et al. 2002. Ethanol elicits and potentiates nociceptor responses via the vanilloid receptor-1. *Nat. Neurosci*. 5:546–551.
32. De Petrocellis, L., S. Harrison, T. Bisogno, M. Tognetto, I. Brandi, G.D. Smith, C. Creminon, J.B. Davis, P. Geppetti, and V. Di Marzo. 2001. The vanilloid receptor (VR1)-mediated effects of anandamide are potently enhanced by the cAMP-dependent protein kinase. *J. Neurochem*. 77:1660–1663.
33. Rathee, P.K., C. Distler, O. Obreja, W. Neuhuber, G.K. Wang, S.Y. Wang, C. Nau, and M. Kress. 2002. PKA/AKAP/VR-1 module: a common link of Gs-mediated signaling to thermal hyperalgesia. *J. Neurosci*. 22:4740–4745.
34. Li, H., B. Degenhardt, D. Tobin, Z.X. Yao, K. Tasken, and V. Papadopoulos. 2001. Identification, localization, and function in steroidogenesis of PAP7: a peripheral-type benzodiazepine receptor- and PKA (RIalpha)-associated protein. *Mol. Endocrinol*. 15:2211–2228.
35. Vijayaraghavan, S., S.A. Goueli, M.P. Davey, and D.W. Carr. 1997. Protein kinase A-anchoring inhibitor peptides arrest mammalian sperm motility. *J. Biol. Chem*. 272:4747–4752.
36. Schagger, H., W.A. Cramer, and G. von Jagow. 1994. Analysis of molecular masses and oligomeric states of protein complexes by blue native electrophoresis and isolation of membrane protein complexes by two-dimensional native electrophoresis. *Anal. Biochem*. 217:220–230.
37. Schamel, W.W., and M. Reth. 2000. Monomeric and oligomeric complexes of the B cell antigen receptor. *Immunity*. 13:5–14.
38. Turner, H., A. Fleig, A. Stokes, J.P. Kinet, and R. Penner. 2003. Discrimination of intracellular calcium store subcompartments using TRPV1 (transient receptor potential channel, vanilloid subfamily member 1) release channel activity. *Biochem. J*. 371:341–350.
39. Nadler, M.J., M.C. Hermosura, K. Inabe, A.L. Perraud, Q. Zhu, A.J. Stokes, T. Kurosaki, J.P. Kinet, R. Penner, A.M. Scharenberg, and A. Fleig. 2001. LTRPC7 is a Mg.ATP-regulated divalent cation channel required for cell viability. *Nature*. 411:590–595.
40. Heiner, I., J. Eisfeld, and A. Luckhoff. 2003. Role and regulation of TRP channels in neutrophil granulocytes. *Cell Calcium*. 33:533–540.
41. Minke, B., and B. Cook. 2002. TRP channel proteins and signal transduction. *Physiol. Rev*. 82:429–472.
42. Rosenbaum, T., M. Awaya, and S.E. Gordon. 2002. Subunit modification and association in VR1 ion channels. *BMC Neurosci*. 3:4.
43. van de Graaf, S.F., J.G. Hoenderop, D. Gkika, D. Lamers, J. Prenen, U. Rescher, V. Gerke, O. Staub, B. Nilius, and R.J. Bindels. 2003. Functional expression of the epithelial Ca(2+) channels (TRPV5 and TRPV6) requires association of the S100A10-annexin 2 complex. *EMBO J*. 22:1478–1487.
44. Kedei, N., T. Szabo, J.D. Lile, J.J. Treanor, Z. Olah, M.J. Iadarola, and P.M. Blumberg. 2001. Analysis of the native quaternary structure of vanilloid receptor 1. *J. Biol. Chem*. 276: 28613–28619.
45. Cesare, P., A. Moriondo, V. Vellani, and P.A. McNaughton. 1999. Ion channels gated by heat. *Proc. Natl. Acad. Sci. USA*. 96:7658–7663.
46. Clapham, D.E., C. Montell, G. Schultz, and D. Julius. 2003. International union of pharmacology. XLIII. Compendium of voltage-gated ion channels: transient receptor potential channels. *Pharmacol. Rev*. 55:591–596.
47. Maingret, F., I. Lauritzen, A.J. Patel, C. Heurteaux, R. Reyes, F. Lesage, M. Lazdunski, and E. Honore. 2000. TREK-1 is a heat-activated background K(+) channel. *EMBO J*. 19:2483–2491.
48. Colledge, M., and J.D. Scott. 1999. AKAPs: from structure to function. *Trends Cell Biol*. 9:216–221.
49. Liu, J., H. Li, and V. Papadopoulos. 2003. PAP7, a PBR/PKA-RIalpha-associated protein: a new element in the relay of the hormonal induction of steroidogenesis. *J. Steroid Biochem. Mol. Biol*. 85:275–283.
50. Biro, T., M. Maurer, S. Modarres, N.E. Lewin, C. Brodie, G. Acs, P. Acs, R. Paus, and P.M. Blumberg. 1998. Characterization of functional vanilloid receptors expressed by mast cells. *Blood*. 91:1332–1340.
51. Lewin, G.R., A. Rueff, and L.M. Mendell. 1994. Peripheral and central mechanisms of NGF-induced hyperalgesia. *Eur. J. Neurosci*. 6:1903–1912.